

Negative yield stress temperature anomaly and structural instability of Pt₃Al

Yu. N. Gornostyrev,^{1,2} O. Yu. Kontsevoi,¹ A. F. Maksyutov,³ A. J. Freeman,¹ M. I. Katsnelson,^{2,4,5}
A. V. Trefilov,³ and A. I. Lichtenshtein⁵

¹*Department of Physics and Astronomy, Northwestern University, Evanston, Illinois 60208-3112, USA*

²*Institute of Metal Physics, 620219 Ekaterinburg, Russia*

³*Russian Science Center "Kurchatov Institute," 123182 Moscow, Russia*

⁴*Department of Physics, Uppsala University, Box 530, SE-751 21 Uppsala, Sweden*

⁵*University of Nijmegen, NL 6525 ED Nijmegen, The Netherlands*

(Received 23 December 2003; published 14 July 2004)

First-principles electronic structure and total energy calculations of the phase stability and dislocation properties of Pt₃Al are employed to reveal the origins of its yield stress low temperature anomaly (LTA). An analysis of the dislocation structure and mobility, based on generalized stacking fault calculations, demonstrates that the LTA is connected with the $L1_2 \rightarrow DO'_c$ structural transformation rather than, as traditionally believed, with features of the dislocation structure in the $L1_2$ phase. We also explain why the yield stress and slip geometry have a strong orientation dependence and why small deviations from stoichiometry lead to dramatic changes in its mechanical behavior.

DOI: 10.1103/PhysRevB.70.014102

PACS number(s): 62.20.Fe, 71.15.Nc, 71.20.Lp

Understanding the relation between dislocation structure and mechanical properties is one of the key problems in materials science. In most solids, the increase of temperature leads to a decrease of the yield stress, σ_y ; this can be naturally explained by the growth of the dislocation mobility due to thermal fluctuations.¹ The opposite behavior, known as the yield stress anomaly (YSA), when $\sigma_y(T)$ increases with temperature, was first discovered in Ni₃Al more than 30 years ago,² and is still a subject of intense research due to its technological importance for high-temperature applications.³

While the YSA takes place in most $L1_2$ intermetallics, there are a few systems, most notably Pt₃X ($X = \text{Al, Ga, Ge}$), where the YSA has not been observed; instead, they demonstrate a very sharp decrease of $\sigma_y(T)$ with increase of temperature at $T < 400$ K.⁴ While a rapid decrease of the yield stress is normal for materials with a high Peierls stress, e.g., in bcc transition metals, it is so highly unusual for $L1_2$ intermetallics that a new term—the low temperature anomaly (LTA)—was introduced by Oya-Seimiya *et al.*⁵ to characterize such a behavior.

The most widely accepted mechanism of the YSA involves thermally activated cross-slip of the $\langle 110 \rangle \{111\}$ superdislocations into the $\{001\}$ plane, where they become immobile as a result of a noncoplanar (sessile) configuration (for a review, see Refs. 6–9). The Paidar-Pope-Vitek (PPV) theory¹⁰ devised a condition for the occurrence of the YSA based on a relation between antiphase boundary (APB) and superlattice intrinsic stacking fault (SISF) energies on the $\{111\}$ shear plane, and the APB energy on the $\{001\}$ plane. In typical $L1_2$ intermetallics (such as Ni₃Al or Ni₃Ge), $\langle 110 \rangle \{111\}$ superdislocations split into superpartials separated by APB ($\langle 110 \rangle \rightarrow \frac{1}{2} \langle 110 \rangle + \text{APB} + \frac{1}{2} \langle 110 \rangle$), which will lead to the YSA provided the $\{001\}$ APB energy is sufficiently low. In alloys with high APB and/or low SISF energies, the superdislocations are dissociated into superpartials separated by SISF ($\langle 110 \rangle \rightarrow \frac{1}{3} \langle 112 \rangle + \text{SISF}$

$+ \frac{1}{3} \langle 112 \rangle$), and this should explain both the lack of the YSA and the presence of the LTA. Paidar *et al.*¹⁰ proposed that Pt₃X alloys belong to the latter category (see also Refs. 8 and 9). The PPV concept is now widely accepted as it gives a plausible explanation of the $\sigma_y(T)$ behavior in $L1_2$ alloys with YSA as well as in some $L1_2$ alloys without a YSA, such as Fe₃Ge.¹¹ However, for Pt₃Al, the results of both experimental investigations of the dislocation structure⁷ and *ab initio* calculations of the stacking fault energies^{12,13} are in contradiction with the mechanism proposed by Paidar *et al.*¹⁰ Namely, the SISF energy is not low but rather larger than the APB energy,¹² and no experimental observations of the SISF-bound $\{111\}$ superdislocations exist. Thus, the true nature of the LTA in Pt₃Al still remains unclear.

In this paper, we present a solution to the problem of the unusual mechanical behavior of Pt₃Al on the basis of *ab initio* electronic structure and total energy calculations of its phase stability and dislocation properties. We employ a theoretical approach which allows us to analyze features of the dislocation structure, energetics, and mobility without the ambiguity caused by the use of semiempirical interatomic potentials in a previous analysis.¹⁰ First, we examine a suggestion⁵ that the anomalous mechanical properties of Pt₃Al are connected with the instability of the $L1_2$ structure with respect to its transformation to DO'_c -type phases. We show that the DO'_c rather than the $L1_2$ structure is a ground state phase in a narrow composition region near stoichiometry. For the first time, we determine the dislocation structure in $L1_2$ and DO'_c Pt₃Al on the basis of *ab initio* generalized stacking fault calculations. The LTA is demonstrated to be connected with the structural instability rather than with features of the dislocation structure of the $L1_2$ phase, as traditionally believed. Based on our calculated results, we explain why the yield stress strongly depends on the orientation of the deformation axis with respect to the orientation of the Pt₃Al single crystal,¹⁴ and why small deviations

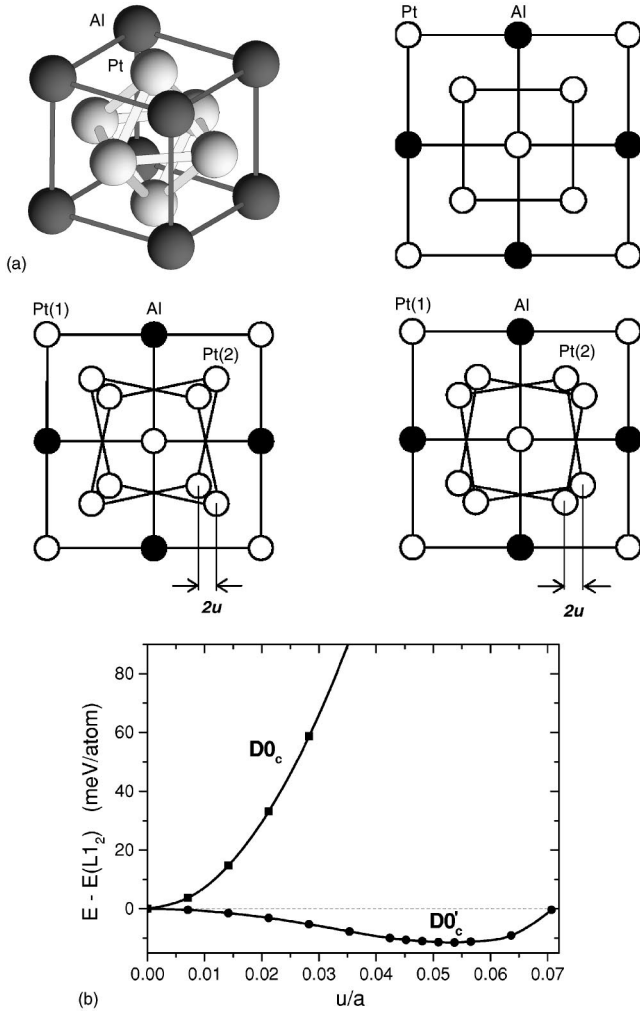


FIG. 1. (a) $\{001\}$ projections of $L1_2$, $D0_c$, and $D0'_c$ structures; (b) energy difference $E - E(L1_2)$ as a function of the displacement u for $D0_c$ and $D0'_c$ structures.

from stoichiometry lead to dramatic changes of the mechanical behavior of Pt_3Al and to the disappearance of the LTA.⁵

First-principles electronic structure and total energy calculations for Pt_3Al in its $L1_2$, $D0_c$, and $D0'_c$ phases were performed by the all-electron full-potential linearized augmented plane wave (FLAPW) method¹⁵ without any shape approximation for the potential and charge density. The generalized gradient approximation (GGA) within the Perdew-Burke-Ernzerhof functional was used for the exchange-correlation potential.¹⁶

In the $L1_2$ structure, Pt atoms form octahedra, and the $D0_c$ and $D0'_c$ structures can be obtained by monotonic transformations of the $L1_2$ in such a way that Pt octahedra become either distorted ($D0_c$), or rotated ($D0'_c$), with the distortion parameter u [cf. Fig. 1(a)]. These transformations are also accompanied by a tetragonal distortion of the lattice. From total energy calculations for stoichiometric Pt_3Al , we found that the $D0'_c$ structure is energetically preferable in comparison with the $L1_2$ phase [Fig. 1(b)], with values of u equal to $0.054a$ (where a is the $L1_2$ lattice constant). In contrast, the $D0_c$ structure was found to be unstable for any

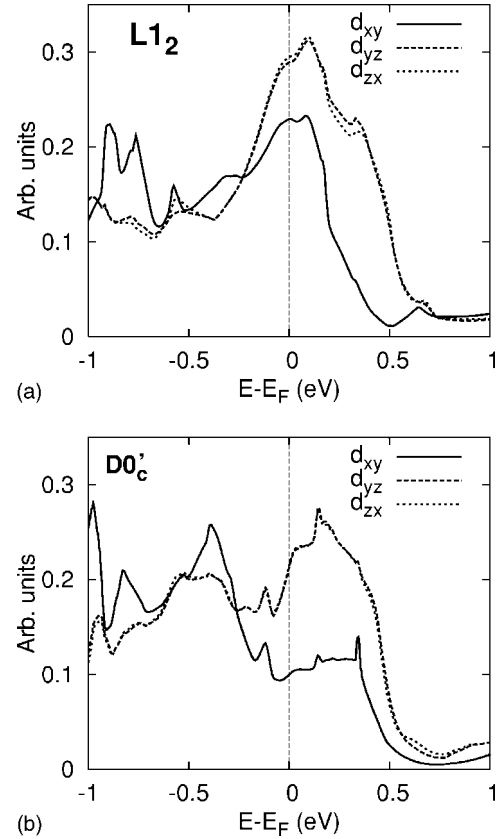


FIG. 2. Orbital contributions to Pt(2) d -DOS for Pt_3Al in the (a) $L1_2$ and (b) $D0'_c$ structures.

value of u (Fig. 1). The calculated lattice parameters were found to be in a good agreement with available experimental data.^{17,18} According to Ref. 18 the magnitude of the crystal lattice distortions decreases gradually with increasing temperature, and disappears above $T = 350$ K. Thus, within the temperature region where the LTA is observed, Pt_3Al has the $D0'_c$ structure.

Our computational results clearly show that the instability of the $L1_2$ structure has an electronic origin. The electronic structure of this phase is characterized by the presence of a peak in the density of states (DOS) exactly at the Fermi level, E_F [cf. Fig. 2(a)], which is an indication of a structural instability that can lead to an essential softening of the lattice (both phonons and elastic moduli); for a review see Ref. 19. Normally, the instability is relieved by either the onset of magnetism or by a transformation into a different structure. In the case of Pt_3Al , the $DOS(E_F)$ is too small to satisfy the Stoner criterion of magnetism. Instead, a martensitic structural transformation is sufficient to stabilize the structure by means of the rotation of Pt octahedra. The DOS peak at E_F is formed mostly by the Pt d states with t_{2g} symmetry, namely d_{xy} orbitals and twofold-degenerate d_{yz} and d_{xz} orbitals. Under the transition to the $D0'_c$ phase, the DOS value at E_F decreases [cf., Fig. 2(b)], and E_F falls at the local minimum in the DOS. Now, because of the unequal population of the three orbitals forming the DOS peak, the charge distribution in the $D0'_c$ phase becomes more anisotropic (“covalent”), as shown in Fig. 3. One can see that additional electron density

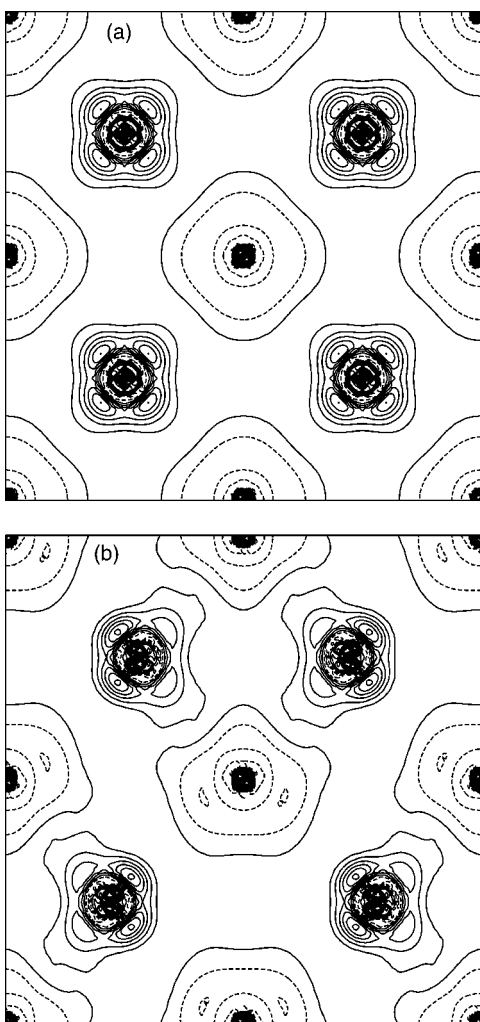


FIG. 3. Charge density difference distribution on the $\{100\}$ plane for Pt_3Al in (a) $L1_2$ and (b) $D0'_c$ phases.

“bridges” are formed between neighboring Pt and Al atoms which enhances their chemical bonding. The appearance of these bonds makes the $D0'_c$ structure stable and energetically favorable.

A close consideration of the LDOS in Fig. 2(a) reveals that in the framework of a rigid band approximation one could expect that a small deviation from stoichiometry should change the number of electrons in the valence band and effectively push E_F away from a local maximum, thus stabilizing the $L1_2$ structure. To investigate the effects of nonstoichiometry on the electronic structure, we modeled the $\text{Pt}_{3-x}\text{Al}_{1+x}$ alloys with a 32-atom supercell, where the substitution of one or two Pt atoms by Al corresponds to the compositions $x=3.125$ or $x=6.25$ at. %, respectively. We found that an excess of Al leads to a monotonic decrease of the energy difference, ΔE , between the $D0'_c$ and the $L1_2$ phases. Simultaneously, the displacement parameter u decreases, and the Pt octahedra rotate back to the original positions which they had in the $L1_2$ structure. The $L1_2$ phase becomes energetically preferable at 6 at. % excess Al (Table I). Thus, the addition of Al stabilizes the $L1_2$ phase—as a consequence of moving the DOS peak off E_F ; a similar mechanism of the

TABLE I. Dependence of the energy difference between the $L1_2$ and $D0'_c$ structures and the displacement parameter u on the composition of $\text{Pt}_{3-x}\text{Al}_{1+x}$.

Composition	$E(L1_2) - E(D0'_c)$ (meV/at.)	u/a
$\text{Pt}_{75}\text{Al}_{25}$	11.5	0.054
$\text{Pt}_{72}\text{Al}_{28}$	4.3	0.035
$\text{Pt}_{69}\text{Al}_{31}$	-0.4	0.014 ^a

^aThe $D0'_c$ structure is metastable.

effect of doping on the phase stability was considered for the case of NiTi.²⁰

The displacements transforming the $L1_2$ into the $D0'_c$ structure move part of the Pt atoms out of the $\{111\}_{L1_2}$ plane and destroy the close packing of the atoms in these layers. As a result, the $\{111\}$ deformation mode which usually operates in $L1_2$ alloys, may become unfavorable in the $D0'_c$ phase. Now, for the analysis of the dislocation structure and mobility we employ a combined approach based on *ab initio* calculations of the generalized stacking fault (GSF), or γ surface, energetics and the two-dimensional (2D) Peierls-Nabarro (PN) model.^{11,21–24} This approach was previously successfully applied by us to analyze the dislocation structure and mechanical behavior of various metals and intermetallics in different structures, including fcc,²² B2,²³ $L1_0$,²⁴ and $L1_2$.¹¹ In order to determine the GSF energies, which are associated with a rigid shift of one part of the crystal with respect to another on an arbitrary fault vector in the slip plane,²⁵ we carried out first-principles total energy FLAPW calculations within the GGA using a supercell geometry with six atomic layers and homogeneous periodic boundary conditions.¹²

First, we consider Pt_3Al in the (hypothetical) $L1_2$ structure. Total energy calculations show that the γ surface on a $\{111\}$ slip plane [Fig. 4(a)] and, in particular, the stacking fault energies (cf. Table II) are very similar to those for Ni_3Ge ,¹¹ which is an intermetallic with a well-pronounced YSA. However, in contrast to Ni_3Ge , the APB energy in the $\{001\}$ plane is very high and $E(\text{APB}_{\{001\}}) \approx E(\text{APB}_{\{111\}})$. This result is in agreement with previous calculations¹³ and distinguishes Pt_3Al from most other $L1_2$ alloys, where the condition $E(\text{APB}_{\{001\}}) < E(\text{APB}_{\{111\}})/\sqrt{3}$ is satisfied;¹² the latter is considered as a necessary requirement for YSA.^{6,7} Since the high value of $E(\text{APB}_{\{001\}})$ prevents cross-slip of the dislocation into the $\{001\}$ (“cube”) plane, $L1_2$ Pt_3Al would not exhibit the YSA. And because the APB-bound $\langle 110 \rangle \{111\}$ superdislocations have a significantly lower Peierls stress¹⁰ than the $\langle 110 \rangle \{001\}$ superdislocations, one could expect that only the $\langle 110 \rangle \{111\}$ slip mode would operate. These results clearly demonstrate that the LTA, which is a result of the dislocation glide on a cube plane $\langle 110 \rangle \{001\}$,²⁷ is not a property of the $L1_2$ Pt_3Al .

The situation changes dramatically when we consider Pt_3Al in the $D0'_c$ structure. In this case, the γ surface is substantially different from that for the $L1_2$ structure [Fig. 4(b)]. First, all stacking fault energies are significantly higher (Table II). In addition, due to the lowering of the

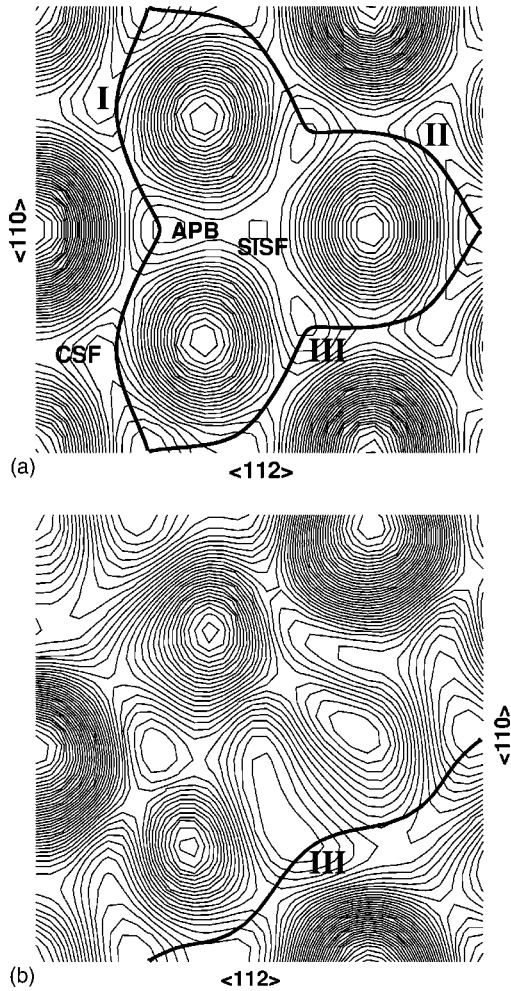


FIG. 4. Contour plots of the generalized stacking fault energies for Pt_3Al with (a) $L1_2$ and (b) $D0'_c$ structures. Structures of superdislocations are shown as “splitting paths” (Ref. 24) (bold lines). Three superdislocations with the APB ribbon can operate on $\{111\}$ slip planes in the $L1_2$ structure and only one (for the easy direction) for $D0'_c$.

lattice symmetry, the displacements in the three $\langle 110 \rangle$ directions [and corresponding APB and complex stacking fault (CSF) energies] which are equivalent in the $L1_2$ structure, become different. As a result, there are two “hard” (I, II) shear directions where the APB energies are twice as large as in an “easy” direction (III) (cf. Table II). Therefore the properties of the dislocations should differ significantly for $\langle 110 \rangle$ Burgers vectors parallel to the hard and easy directions.

The structure of the superdislocations obtained in the framework of our *ab initio* PN approach, is shown in Fig. 4 as a “splitting path,” which gives the dependence of the edge component along the $\langle 112 \rangle$ direction on the screw component along the $\langle 110 \rangle$ direction of the displacement. We found that for (hypothetical) $L1_2$ Pt_3Al , the splitting of the superdislocation through the SISF is highly unfavorable; this confirms the results of the above analysis based on stacking fault energies alone. Only superdislocations split through the APB can operate in $L1_2$ Pt_3Al [Fig. 4(a)].

TABLE II. Energies of unrelaxed geometrical stacking faults: antiphase boundary (APB), complex stacking fault (CSF), and superlattice intrinsic stacking fault (SISF), in mJ/m^2 .

Stacking fault		$\text{Pt}_3\text{Al}(D0'_c)$	$\text{Pt}_3\text{Al}(L1_2)$	$\text{Ni}_3\text{Ge}(L1_2)$
$\text{APB}_{\{111\}}$	(I)	1160		
	(II)	1160	480	660 (Ref. 11)
	(III)	550		
CSF	(I)	1500		
	(II)	780	560	620 (Ref. 11)
	(III)	640		
SISF		780	490	420 (Ref. 11)
$\text{APB}_{\{001\}}$		840	460	300 (Ref. 26)

In $D0'_c$ Pt_3Al , the picture will be similar if the Burgers vector lies along the easy direction [Fig. 4(b)]. For hard directions, however, the superdislocations have compact cores because of the very high APB energy $E(\text{APB}_{\{111\}})$. As a result, superdislocations in the $\{001\}$ cube plane, with lower APB energy $E(\text{APB}_{\{001\}})$, will be energetically more preferable. Although the condition $E(\text{APB}_{\{001\}}) < E(\text{APB}_{\{111\}})$ is fulfilled for hard directions, it does not lead to the YSA because the cube glide $\langle 110 \rangle \{001\}$, which is usually observed in Pt_3Al , naturally appears as a main slip system in the $D0'_c$ structure. Therefore, the LTA, which results from cube dislocation glide,^{9,10} is a property of Pt_3Al in the $D0'_c$ phase and not in the $L1_2$ phase.

Because of the large anisotropy of the shear resistance in $D0'_c$ Pt_3Al , both slip planes— $\{111\}$ for the easy and $\{001\}$ for the hard direction of the Burgers vector—can operate in this alloy depending on the orientation of the deformation axis. This is in agreement with experiment,¹⁴ where slip on only one $\{111\}$ system was observed in Pt_3Al single crystals and only when the deformation axis was oriented near the $\langle 001 \rangle$ direction, while the $\{001\}$ slip prevailed at most other orientations. Since the relative stability of the $D0'_c$ and the $L1_2$ structures is very sensitive to deviations from stoichiometry, and since different deformation modes operate in these two phases, one predicts that the deformation behavior can change drastically with increasing Al concentration. This was actually observed in experiments.⁵ We also predict that at elevated temperatures ($T > 400$ K), where the $L1_2$ structure becomes more favorable,¹⁸ the switch from $\{001\} \langle 110 \rangle$ to $\{111\} \langle 110 \rangle$ slip modes should occur.

To conclude, our results show that the relatively small atomic displacements that accompany the $L1_2 \rightarrow D0'_c$ transition lead to drastic changes in γ -surface energetics and in the mechanical behavior of Pt_3Al . The instability of the $L1_2$ structure has an electronic origin, and similar behavior is expected for other platinum-based intermetallics. Thus, a proper consideration of the structural stability is a key element in explaining the absence of the YSA in $L1_2$ intermetallics—namely, the $L1_2 \rightarrow D0'_c$ (in Pt_3X), or the $L1_2$

→ $D0_{19}$ transformation [in Zr_3Al and Fe_3Ge (Ref. 11)]. The predicted features of the dislocations in $D0'_c$ could be verified experimentally by transmission electron microscopy and slip system investigations.

This work was supported by the AFOSR under Grant No. F49620-01-1-0166, by computer time grants at NCSA and NAVO, and in part by the Netherlands Organization for Scientific Research (NWO Project No. 047-008-16).

-
- ¹J. Friedel, *Dislocations* (Pergamon Press, New York, 1964).
 - ²J. H. Westbrook, *Trans. Am. Inst. Min., Metall. Pet. Eng.* **209**, 898 (1957).
 - ³D. G. Backman and J. C. Williams, *Science* **255**, 1082 (1992).
 - ⁴D. M. Wee, O. Noguchi, Y. Oya, and T. Suzuki, *Trans. Jpn. Inst. Met.* **21**, 237 (1980).
 - ⁵Y. Oya-Seimiya, T. Shinoda, and T. Suzuki, *Mater. Trans., JIM* **37**, 1464 (1996).
 - ⁶D. P. Pope, in *Physical Metallurgy*, edited by R. W. Cahn and P. Haasen (North-Holland, Amsterdam, 1996), Vol. III, p. 2075.
 - ⁷P. Veysiere and G. Saada, in *Dislocations in Solids*, edited by F. R. N. Nabarro and M. S. Duesbery (North-Holland, Amsterdam, 1996), Vol. 10, p. 254.
 - ⁸V. Vitek, *Intermetallics* **6**, 579 (1998).
 - ⁹V. Vitek, D. P. Pope, and J. L. Bassani, in *Dislocations in Solids*, edited by F. R. N. Nabarro and M. S. Duesbery (North-Holland, Amsterdam, 1996), Vol. 10, p. 136.
 - ¹⁰V. Paidar, D. P. Pope, and V. Vitek, *Acta Metall.* **32**, 435 (1984).
 - ¹¹O. N. Mryasov, Yu. N. Gornostyrev, M. van Schilfgaard, and A. J. Freeman, *Acta Mater.* **50**, 4545 (2002).
 - ¹²A. T. Paxton, in *Electron Theory in Alloy Design*, edited by D. G. Pettifor and A. H. Cottrell (Institute of Metals, London, 1992), p. 158.
 - ¹³A. T. Paxton and Y. Q. Sun, *Philos. Mag. A* **78**, 85 (1998).
 - ¹⁴F. E. Heredia, G. Tichy, D. P. Pope, and V. Vitek, *Acta Metall.* **37**, 2755 (1989).
 - ¹⁵E. Wimmer, H. Krakauer, M. Weinert, and A. J. Freeman, *Phys. Rev. B* **24**, 864 (1981).
 - ¹⁶J. P. Perdew, K. Burke, and M. Ernzerhof, *Phys. Rev. Lett.* **77**, 3865 (1996).
 - ¹⁷T. Chattopadhyay and K. Schubert, *J. Less-Common Met.* **41**, 19 (1975).
 - ¹⁸W. Bronger, K. Wrzesien, and P. Müller, *Solid State Ionics* **101-103**, 633 (1997).
 - ¹⁹S. V. Vonsovsky, M. I. Katsnelson, and A. V. Trefilov, *Phys. Met. Metallogr.* **76**, 247 (1993).
 - ²⁰V. I. Anisimov, M. I. Katsnelson, A. I. Lichtenstein, and A. V. Trefilov, *Pis'ma Zh. Eksp. Teor. Fiz.* **45**, 285 (1987).
 - ²¹B. Joos, Q. Ren, and M. S. Duesbery, *Phys. Rev. B* **50**, 5890 (1994).
 - ²²Yu. N. Gornostyrev, M. I. Katsnelson, N. I. Medvedeva, O. N. Mryasov, A. J. Freeman, and A. V. Trefilov, *Phys. Rev. B* **62**, 7802 (2000).
 - ²³N. I. Medvedeva, O. N. Mryasov, Yu. N. Gornostyrev, D. L. Novikov, and A. J. Freeman, *Phys. Rev. B* **54**, 13506 (1996).
 - ²⁴O. N. Mryasov, Yu. N. Gornostyrev, and A. J. Freeman, *Phys. Rev. B* **58**, 11927 (1998).
 - ²⁵V. Vitek, *Cryst. Lattice Defects* **5**, 1 (1974).
 - ²⁶T. J. Balk, M. Kumar, and K. J. Hemker, *Acta Mater.* **49**, 1725 (2001).
 - ²⁷D.-M. Wee, D. P. Pope, and V. Vitek, *Acta Metall.* **32**, 829 (1984).